JVSTB
JOURNAL OF VACUUM SCIENCE AND TECHNOLOGY B

Sensing properties of infrared nanostructured plasmonic crystals fabricated by electron beam lithography and argon ion milling

Baogang Quan, Zhe Liu, Lin Li, Weijie Sun, Xinlong Xu et al.

Citation: J. Vac. Sci. Technol. B 30, 06FE02 (2012); doi: 10.1116/1.4767274

View online: http://dx.doi.org/10.1116/1.4767274

View Table of Contents: http://avspublications.org/resource/1/JVTBD9/v30/i6

Published by the AVS: Science & Technology of Materials, Interfaces, and Processing

Sensing properties of infrared nanostructured plasmonic crystals fabricated by electron beam lithography and argon ion milling

Baogang Quan, Zhe Liu, Lin Li, Weijie Sun, Xinlong Xu, Xiaoxiang Xia, Haifang Yang, Junjie Li,[a] and Changzhi Gu[b]
Beijing National Laboratory for Condensed Matter Physics, Institute of Physics, Chinese Academy of Science, Beijing 100080, China

(Received 29 June 2012; accepted 29 October 2012; published 26 November 2012)

In this paper, the authors report on the fabrication, theory simulation, and optical characterization of X-shaped nanoscale plasmonic crystals (PCs) and their application in biosensors. X-shaped PCs with 30 nm feature line-widths and different intersection angles were fabricated by a combination of electron beam lithography and argon ion beam milling techniques. Both experimental measurement and finite-difference time-domain simulations were employed to study the transmission properties of PCs under two different incident light polarizations. With the reduction of the symmetry of the X-shaped PCs, the transmission spectra of PCs show a new peak at ~900 nm in the near-infrared region, and the optical experimental results were consistent with the simulated results. Plasmonic crystal-based biosensors were then prepared by self-assembly of octadecanethiol to the PCs followed by biotinylation and immobilization of streptavidin to the biosensor. The sensing properties of the PC-based biosensors with a 30° intersection angle, which is enhanced by a localized surface plasmon resonance with the asymmetry of the PC, are superior to those with a larger intersection angle in biosensor application. The robust fabrication technique and the strategy for enhancing the sensitivity of the biosensor endow X-shaped PCs with a great competitive advantage over other candidates. © *2012 American Vacuum Society*. [http://dx.doi.org/10.1116/1.4767274]

I. INTRODUCTION

A plasmonic crystal (PC) is a kind of artificial material consisting of a nanostructured noble metal film which exploits surface plasmon polaritons (SPPs) and is a family member of metamaterials.[1–3] The past two decades have witnessed the emergence and rapid growth of metamaterials due to the recent progress of micro- and nanofabrication technologies. As a consequence, the concepts of negative index, chiral metamaterials, and artificial magnetism have been widely accepted. Now the focus of research has moved into the domain of application, and PC-based sensors for the purpose of detection of biological and chemical molecules are listed as one of the emerging directions of the investigation of metamaterials.[4]

Surface plasmon resonance (SPR), which is a collective free electron oscillation stimulated by the incident light at the metal/dielectric interface of PCs, enables chemical and even label-free biological sensing. Since surface plasmons are strongly confined at the metal surface, they are very sensitive to changes in the dielectric properties of the interface. Although happening in the vicinity of the metal surface, the information about the near-field interaction of the surface plasmons with the analytes can be carried by far-field light transmitted from the PC. Typically, transmission intensity variation and/or the frequency shift of the transmission spectrum were utilized to implement SPR-based sensors.[5–7] The enhancement of the transmission of PC-based sensors is widely accepted as a result of the SPPs and the localized surface plasmon resonances. Localized surface plasmon resonances are SPRs generated by a light wave interacted with nanostructures smaller than the wavelength of light. Size, shape, density, and periodicity of nanostructures have significant effects on the localized surface plasmon resonance. Though localized surface plasmon resonance is dominated by the shape and asymmetric parameters of holes in PCs,[5,8] there are few experimental and theoretical reports about asymmetric-effect enhancement of the transmission of PCs.[9–11] Infrared (IR) PCs are especially important for biosensing applications because biomolecules possess a mid-infrared fingerprint that can be used for their identification.

On the other hand, it is challenging to fabricate PCs with a feature size scaled down to one tenth of the visible and IR wavelength. Nowadays, the combination of electron beam lithography (EBL) and the lift-off process has been one of the most widely used techniques for the fabrication of optical PCs sensors. Unfortunately, the performance of sensors is influenced significantly by the defects of nanostructures introduced during the lift-off process. To lower the Ohmic losses at visible and near-IR frequencies, defect-free PC structures are necessary. A narrow line-width is also requisite for obtaining large-field enhancements over the surface of PCs, and for optical and IR sensors the line-width of the PC nanostructure is far below 100 nm, which makes the fabrication of high-quality sensors more challenging.

Herein, a series of IR PCs with varying degrees of asymmetry were fabricated by a combination of EBL and ion beam milling processes to fulfill the fabrication of IR PCs. The implementation of symmetry reduction relies on reducing the intersection angle of X-shaped PCs, and the

[a]Electronic mail: jjli@iphy.ac.cn
[b]Electronic mail: czgu@iphy.ac.cn

transmission and biosensing properties were measured. It is found that the intensities of the transmission peak depend strongly on the asymmetry of the X-shaped PCs. The finite-difference time-domain (FDTD) method was used to simulate the electromagnetic response of the PC, which was found to be in good agreement with the experimental result. A self-assembly monolayer of octadecanethiol (ODT) and biotin was immobilized on the gold nanostructures by soaking the PCs in solutions of ODT and biotin in chronological sequence. The PC-based sensor with a 30° intersection angle possesses the highest sensing ability of the binding event of streptavidin and biotin in the near-IR region.

II. EXPERIMENT

A. PC fabrication

As we aimed to fabricate PCs which will response at near infrared region, the length and line-width of the arms, which should be much smaller than the radiated wavelength of infrared light, and the film thickness (30 nm) were chosen by FDTD simulations. The width and length of the arms of the X-shaped PCs studied in this paper were designed to be 30 and 240 nm, respectively, with a lattice constant of 400 nm where the only difference among these PCs is the intersection angle of the two arms. To reduce the defect density and shrink the line-width of the PCs, ion beam etching was used as an alternative to the lift-off process. The fabrication process, which is a combination of EBL and ion beam milling processes, is shown schematically in Fig. 1(a). The pattern was laterally defined by standard EBL on a flat fused quartz plate where the quartz substrates were first sputtered with a gold thin film layer with a thickness of 30 nm to decrease the charging effect. Prior to deposition, the quartz plates were immersed sequentially in acetone, isopropyl alcohol, and deionized water in an ultrasonic bath, with each step performed for 10 min, and then blown dry with nitrogen. Then commercial electron beam resist, polymethylmethacrylate (2% PMMA 950, Microchem), was spin-coated at 4000 rpm and baked at 180 °C for 1 min on a hot plate, with a final film thickness of about 60 nm. A Raith 150 EBL system was used to define the patterns and, after development, the patterned samples were mounted on a rotating sample stage which was tilted in a certain angle and were etched by an ion beam milling system (LKJ-150, Beijing Institute of Advanced Ion Beam Technology). To ensure a clear Au surface on the PC, the sample was cleaned by oxygen plasma (PVA TePla, PS210) for 10 min under the power (600 W) to remove the residual PMMA resist.

Figures 1(b)–1(e) are scanning electron microscope (SEM) images of PCs with different intersection angles of 30° (B), 45° (C), 60° (D), and 90° (E), respectively. Scale bars in the SEM images are 1 μm. The "atoms" of the PCs are arranged into periodic arrays and the lattice constant is 400 nm. The pattern seems fairly uniform with the slit line-width being around 30 nm in all PCs with larger intersection angles except for a slight deformation of the shape of the slit in the PC with a 30° intersection angles. This shape deformation is caused partly by electron repulsion during the lithography process and partly by the grain of the Au film during the etching process.

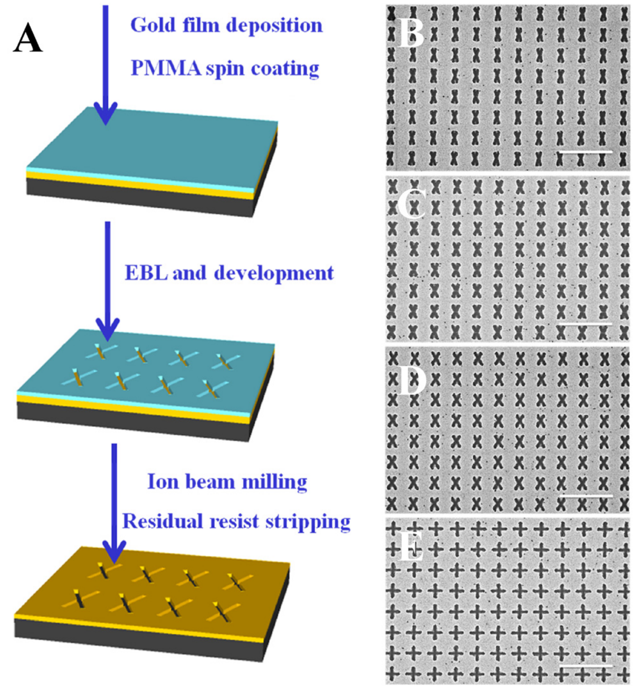

FIG. 1. (Color online) (a) Schematic diagram of the fabrication process of PCs. The substrate is quartz with a thickness of 0.5 mm, which was coated with a 30 nm gold by sputtering. Then, a thin film of (60 nm) PMMA was spin-coated on the substrate. (b)–(e) are SEM images of PCs with different intersection angles 30° (b), 45° (c), 60° (d), and 90° (e), and with a period p = 400 nm, unit length l = 240 nm, and a line-width w = 30 nm. Scale bars in the SEM images are 1 μm.

B. Measurement and FDTD simulation of PC transmission properties

Transmission measurements of PCs and PC-based biosensors were carried out at room temperature using a home-made integrated microscope-spectrometer system under two incident polarizations (0° and 90°) to obtain the transmission spectra. The polarizations were defined with the E-field of the incident light parallel (0° polarization) or perpendicular (90° polarization) to the symmetrical axis which is located in the shape corners of the PC unit, as shown in Fig. 2(c). The system includes a spectrometer iHR-320 from HORIBA Jobin-Yvon, an OLYMPUS BX51 microscope, and detectors. A 100× objective lens, with a numerical aperture of 0.85, was used to collect the enhanced far-field light transmitted through the slit of each PC sample, then the light was dispersed by a monochromator with three selectable gratings of the iHR-320 spectrometer and then detected by a two-channel detector.

To simulate the transmission spectra of PCs, we employed the FDTD method using a flexible free-software package MEEP.[12] In the simulations, the Drude–Lorentz model was used to describe the dispersion of the gold film, the grid size of the FDTD calculation was 1 nm, and the PC structure was placed on a semi-infinite quartz substrate with a refractive index of 1.46.

C. Biosensor preparation and sensing properties

To examine the feasibility of this plasmonic crystal biosensor for label-free biosensing, we employed the biotin–

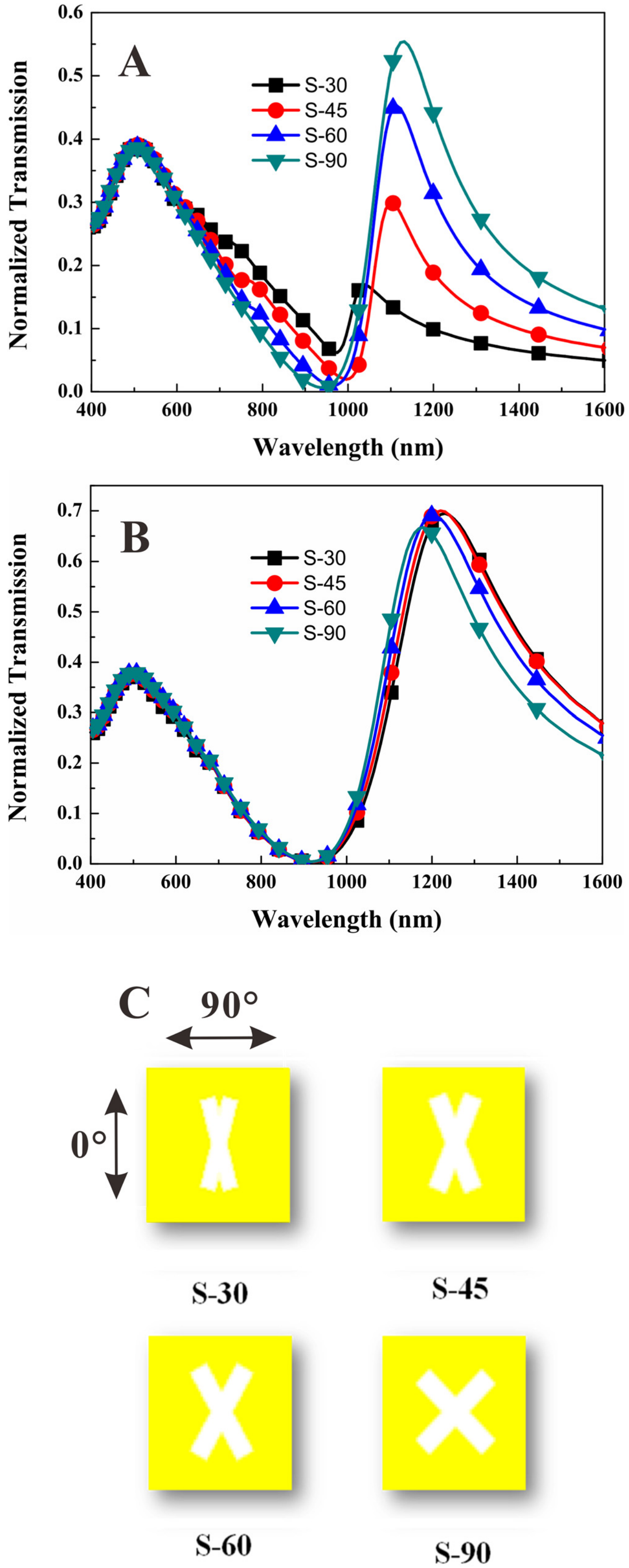

FIG. 2. (Color online) FDTD simulation of the transmission properties of PCs under two different incident light polarizations (0° and 90°). (a) Transmission spectra of PCs under 0° polarization; (b) Transmission spectra of PCs under 90° polarization. (c) The configuration used in the FDTD simulation. The labels (S-30, S-45, S-60, and S-90) of spectra in (a) and (b) are the short forms of samples with intersection angles of 30°, 45°, 60°, and 90°, respectively.

streptavidin binding model. Biotin, ODT, and streptavidin were purchased from Sigma-Aldrich Chemicals and used as obtained without further purification. The functionalization and biorecognition taking place on the PC-based biosensor are simplified into three steps (i.e., ODT functionalization, biotinylation, and streptavidin immobilization), as shown in Fig. 3. As the PC surface is a nanoconstructed gold film, it is easy to functionalize the surface with an alkanethiol self-assembled monolayer (SAM). The stability, uniform surface

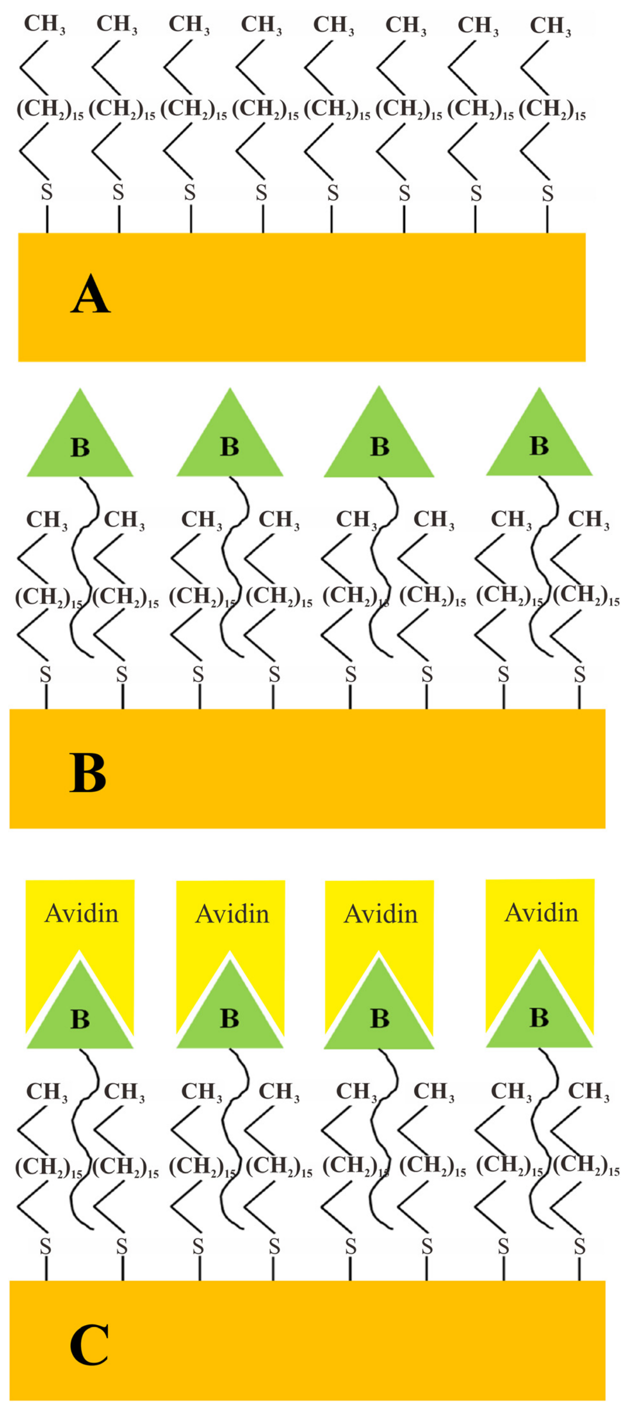

FIG. 3. (Color online) Schematic diagram of biosensor preparation processes. (a) ODT functionalization: the self-assembled monolayer of ODT on gold film, (b) biotinylation: the immobilization of biotin to ODT SAM, and (c) immobilization of streptavidin with biotin.

structure, and relative ease of varying the functionalities have made SAMs of alkanethiols suitable matrices for fabrication of PC-based biosensors. Moreover, the immobilization of biomolecules using a SAM-functionalized surface requires only a small amount of biomolecules and results in the binding of the desired molecule in the near vicinity of the gold surface. In order to get a well-ordered SAM, ODT, a long-chain alkanethiol, was used. As-fabricated PC samples were rinsed in ethanol for 5 min and dried under a stream of dry nitrogen to remove dust from the surface and then the samples were immersed in a 5 mM ODT solution in ethanol. To get a uniform and stable SAM on the surface of our samples, the PC was soaked overnight in the ODT solution at room temperature.

Biotinylation of the Au surface was achieved by immersing the ODT-SAM-functionalized PC in a 5 mM solution of biotin in a phosphate buffer solution for 2 h at room temperature. The terminal alkane chain of the ODT-functionalized samples guaranteed a certain level of stability for the ODT-biotin complexes. To eliminate the effect of nonspecific interactions, the biotinylated PCs were placed in a phosphate buffer solution for 30 min, rinsed with deionized water, and dried with a stream of nitrogen gas. Streptavidin immobilization on the biotinylated surface was achieved by exposing the samples to a 0.1 mg/ml solution of steptavidin in a phosphate buffer solution for 2 h at room temperature. After the immobilization of streptavidin, the samples were rinsed in a phosphate buffer solution for 5 min to wash off the physisorbed streptavidin molecules, and dried under a stream of nitrogen gas.

For investigating the sensing property of the biosensor, the transmission measurements were carried out after biotinylation and streptavidin immobilization of the PC-based biosensors. Transmission spectra of PC-based biosensors were taken with the same microscope-spectrometer system used for the transmission measurement of the PC. The illuminating light emitted from a Halogen lamp was then polarized and made to be normally incident to the surface of the PC-based biosensor via a condenser lens and finally collected with an objective lens ($100\times$, NA $= 0.85$). The transmission spectra of PC-based biosensors were taken under 0° polarization, as defined in subsection B. All transmission spectra were normalized to a reference spectrum taken on the bare part of the flat fused quartz plate under identical conditions to obtain the transmittance of the biosensors.

III. RESULTS AND DISCUSSION

The SEM images of the X-shaped PCs shown in Fig. 1 indicate that the combination of EBL and argon ion beam milling has advantages over other fabrication strategies in that no defects such as line-width and shape deformations were introduced during the fabrication process. For the fabrication of PCs in visible and near-IR frequencies, etching instead of lift-off is a more suitable pattern transfer technique. A slight shape deformation of the PC with a 30° intersection angle is unavoidable because the electron repulsion, caused by the charging effect of the insulating substrate, becomes more significant in the case of direct writing of denser structures using an electron beam.

To evaluate the effect of asymmetry on the transmission properties of PCs with different intersection angles, we measured and calculated the normal incidence transmission spectra of these PCs. Figures 2(a) and 2(b) present the transmission spectra of the PCs under two incident polarizations (0° and 90°) simulated by FDTD, respectively, and the schematic diagram on the top-right corner on Fig. 2 shows the configuration of the polarizations and the PCs. From the FDTD simulation results in Fig. 2, we can see that the transmission spectra of an orthogonally crossed PC (with a 90° intersection angle) under two polarizations are identical. This indicates that symmetry of a cruciform shape endows the orthogonally crossed PC with the ability to respond independent of polarization for normal incidence. Results from an experimental and theoretical study of a multilayer cruciform-shaped metamaterial by Helgert *et al.*[13] point to the same conclusion. With the reduction of the symmetry of the X-shaped PCs, the transmission spectra of PCs with acute intersection angles under 0° polarization become distinct from those of 90° polarization. The peaks located at 500 and 1100 nm are identified as general light transmission of the relatively thin film of gold and enhanced transmission attributed to the resonances of SPPs, respectively. The appearance of peaks at 700–800 nm in the spectra of PCs with increasing asymmetry is believed to be as a consequence of resonance of localized surface plasmon modes. The resonance of localized surface plasmon modes is sensitive to the shape of the hole, and is therefore also called shape-resonance. Though the localized surface plasmon mode is confined to the surface, its contribution can be detected from far-field especially when the electric field of the incident light is parallel to the long axis of the slit. This is the reason for the absence of the peaks in the corresponding region of the spectra of PCs under 90° polarization in Fig. 2(b).

Due to the nature of the localized surface plasmon resonance, it is useful to detect the near-field interaction of the absorption of analytes in the vicinity of the metal surface at a range of a few ten or hundred nanometers. From the discussion of the asymmetry-dependent transmission properties of PCs, we found that the localized surface plasmon modulates the far-field transmission spectrum only when the intersection angle of the PC is an acute angle. Therefore, for the purpose of finding a platform for a biosensor we do not need to investigate the transmission properties of orthogonally crossed PCs. The experimental asymmetry-dependent transmission spectra of PCs under 0° and 90° polarizations are shown in Figs. 4(a) and 4(b), respectively. Compared to the simulated spectra in Fig. 2(a), the peak caused by the resonance of the localized surface plasmon mode experiences a red-shift of about 100 nm while the positions of the other two peaks remain unchanged [see spectra in Fig. 4(a)]. The red-shift can be attributed to the difference between the actual line-width and shape and that the model used in the FDTD simulation. Additionally, the imperfection of the gold film can also affect the resonance of the localized surface

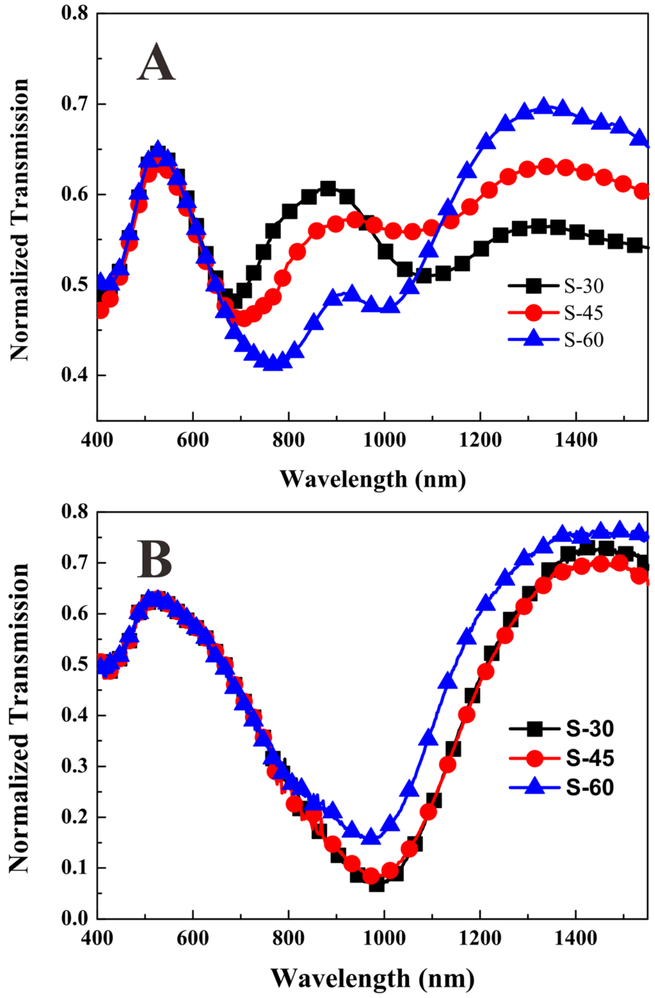

FIG. 4. (Color online) Experimental transmission spectra of PCs. Optical measurements were carried out under 0° (a) and 90° (b) incident polarization.

plasmon and thus broadens the peaks. On the other hand, the experimental transmission spectra of PCs under 90° polarization show remarkable agreement with those in the FDTD simulation.

The biotin–streptavidin biorecognition events of PC-based biosensors are shown in Fig. 5. The green and purple lines represent the transmission spectra of the PC-based biosensor after biotinylation and immobilization of streptavidin, respectively. The sensitivity of the biosensors based on surface plasmon resonance is usually characterized by the change in the environmental refractive index, i.e., the frequency shift or relative intensity variation per refractive index unit.

The intensity difference between the peaks at about 800 nm in the spectra in Fig. 5(c) is fairly large compared with those in Figs. 5(a) and 5(b). This indicates that the intensity variation is a more reliable parameter than frequency shift for detection of the biotin–streptavidin binding event. To quantitatively evaluate the sensing abilities of the biosensors in our work, refractive index sensitivity (S) of the PC-based biosensor was calculated by

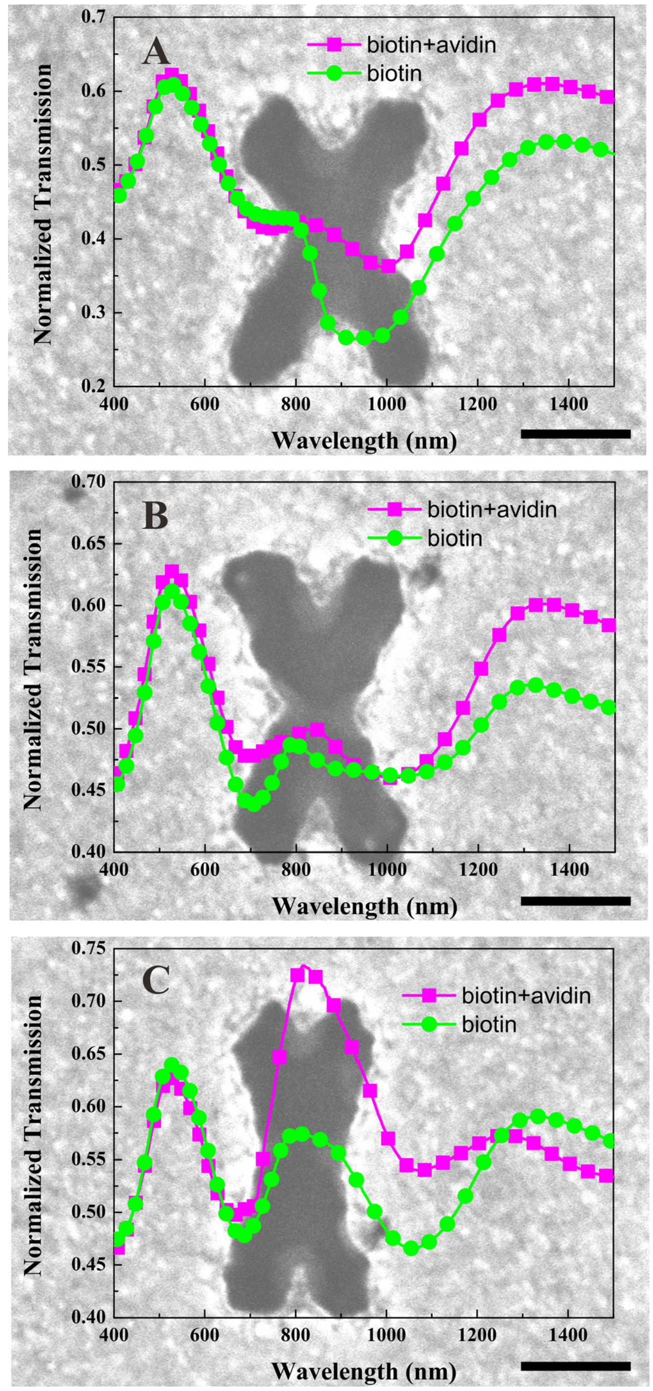

FIG. 5. (Color online) Transmission spectra of the PC-based biosensor after biotinylation (green line) and immobilization of streptavidin (purple line) by the PC-based biosensors with the intersection angle of the two arms being 60° (a), 45° (b), and 30° (c) under incident light at 0° polarization. Scale bars in the SEM images are 100 nm.

$$S = \frac{\Delta I/I_0}{\Delta n} = \frac{\frac{I_{streptavidin} - I_{biotin}}{I_{biotin}} \times 100\%}{n_{streptavidin} - n_{biotin}},$$

where $I_{streptavidin}$ and I_{biotin} are the transmission intensity maxima of streptavidin and biotin at a wavelength of 800 nm, respectively; and $n_{streptavidin}$ and n_{biotin} are the refractive indices of streptavidin and biotin molecules, respectively. We assumed that the biotin molecules have a refractive index of 1.50[14] and streptavidin molecules have a refractive index of 1.57.[15] For the X-shaped biosensor with an intersection of 30°, the relative intensity change is 54.68%, so the refractive index sensitivity is calculated to be 781.1%/RIU at a wavelength of 800 nm, which indicates that the X-shaped biosensor with an intersection of 30° has a rather good performance.

The refractive index sensitivities of PC-based biosensors with intersection angles of 60° and 45° are 17.0%/RIU and 31.6%/RIU, respectively. These results reveal that the PC-based biosensor with a 30° intersection angle is superior to those with larger intersection angles in biosensing. Moreover, it is also evident that the asymmetry of PCs caused by reducing the intersection angle of PC-based biosensors does help to enhance the sensitivity. He *et al.*[16] theoretically studied the transmission characteristics of a metallic film with asymmetric cross-shaped holes, and they found that the transmission spectra can be adjusted by redistribution of the oscillating charges on the metal film caused by changing the geometrical parameters of asymmetric metamaterials. As analyzed above, the intensities of the transmission peaks depend strongly on the asymmetry of the X-shaped PCs when they are measured under 0° incident polarization.

IV. SUMMARY AND CONCLUSIONS

In summary, we have developed a robust fabrication process for high-quality PCs which can respond to light in the visible and IR region by a combination of EBL and argon ion beam milling techniques. The transmission properties of the PCs were investigated by experiment and FDTD simulation with normally incident light under two different polarizations. The experimental and simulated results reveal that the PCs possess a highly sensitive response to the shape and polarization of the incident light. The intensities of the transmission peaks depend strongly on the asymmetric parameters of the cross-shaped hole. With the reduction of the symmetry of the X-shaped PCs, the transmission spectra of PCs show a new peak at the near-IR frequency (900 nm). Then, PC-based biosensors were prepared by self-assembly ODT on the PCs followed by biotinylation and immobilization of streptavidin to biotin. The sensing properties of the PC-based biosensors were studied by comparing the response spectra before and after the immobilization of the streptavidin, and it was found that the PCs with a 30° angle are superior to those with larger intersection angles in biosensor application. Although more optimization work needs to be done, the present results are promising for enhancing the sensitivity of PC-based biosensors.

ACKNOWLEDGMENTS

This work is supported by the National Basic Research Program of China (Grand No. 2009CB930502), the National Natural Science Foundation of China (Grand Nos. 51103175, 61001045, 91023041, 50825206, 10834012, and 11174362), and the Knowledge Innovation Project of CAS (Grand No. KJCX2-EW-W02).

[1] T. T. Truong, J. Maria, J. Yao, M. E. Stewart, T. W. Lee, S. K. Gray, R. G. Nuzzo, and J. A. Rogers, Nanotechnology **20**, 434011 (2009).
[2] M. E. Stewart, N. H. Mack, V. Malyarchuk, J. A. N. Soares, T. W. Lee, S. K. Gray, R. G. Nuzzo, and J. A. Rogers, Proc. Natl. Acad. Sci. U.S.A. **103**, 17143 (2006).
[3] B. Luk'yanchuk, N. I. Zheludev, S. A. Maier, N. J. Halas, P. Nordlander, H. Giessen, and C. T. Chong, Nature Mater. **9**, 707 (2010).
[4] N. I. Zheludev, Science **328**, 582 (2010).
[5] X. L. Xu, B. Peng, D. H. Li, J. Zhang, L. M. Wong, Q. Zhang, S. J. Wang, and Q. H. Xiong, Nano Lett. **11**, 3232 (2011).
[6] J. Feng, V. S. Siu, A. Roelke, V. Mehta, S. Y. Rhieu, G. T. Palmore, and D. Pacifici, Nano Lett. **12**, 602 (2012).
[7] C. W. Wu, A. B. Khanikaev, R. Adato, N. Arju, A. A. Yanik, H. Altug, and G. Shvets, Nature Mater. **11**, 69 (2012).
[8] C. Y. Chen, M. W. Tsai, T. H. Chuang, Y. T. Chang, and S. C. Lee, Appl. Phys. Lett. **91**, 063108 (2007).
[9] A. V. Krasavin, A. S. Schwanecke, and N. I. Zheludev, J. Opt. A, Pure Appl. Opt. **8**, S98 (2006).
[10] A. Roberts and L. Lin, Opt. Lett. **37**, 1820 (2012).
[11] X. M. Goh, L. Lin, and A. Roberts, J. Opt. Soc. Am. B **28**, 547 (2011).
[12] A. F. Oskooi, D. Roundy, M. Ibanescu, P. Bermel, J. D. Joannopoulos, and S. G. Johnson, Comput. Phys. Commun. **181**, 687 (2010).
[13] C. Helgert, C. Menzel, C. Rockstuhl, E. P. Severin, E. B. Kley, A. Chipouline, A. Tunnermann, F. Lederer, and T. Pertsch, Opt. Lett. **34**, 704 (2009).
[14] W. Knoll, M. Zizlsperger, T. Liebermann, S. Arnold, A. Badia, M. Liley, D. Piscevic, F. J. Schmitt, and J. Spinke, Colloids Surf., A **161**, 115 (2000).
[15] L. S. Jung, C. T. Campbell, T. M. Chinowsky, M. N. Mar, and S. S. Yee, Langmuir **14**, 5636 (1998).
[16] M. D. He, J. Q. Liu, Z. Q. Gong, Y. F. Luo, and X. S. Chen, Solid State Commun. **150**, 104 (2010).